

## Electronic Supporting Information

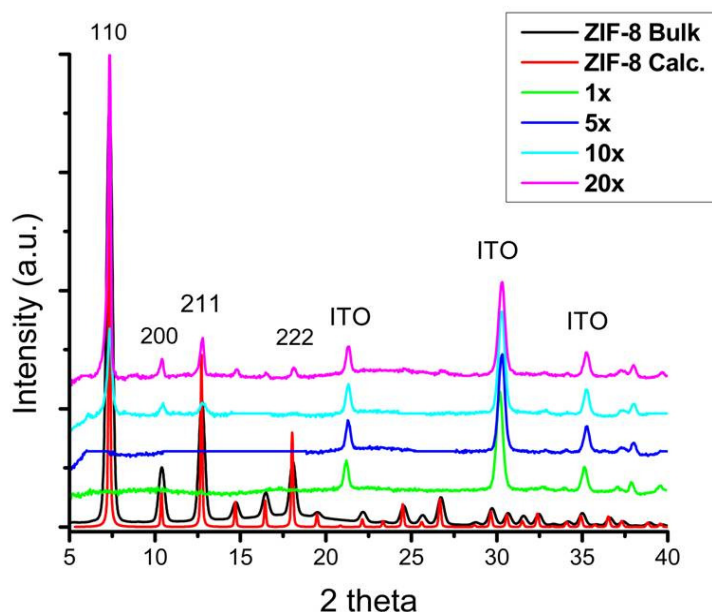
### Early stages of ZIF-8 film growth: the enhancement effect of primers exposing sulfonate groups as surface-confined nucleation agents.

Jimena Tuninetti, Matías Rafti and Omar Azzaroni

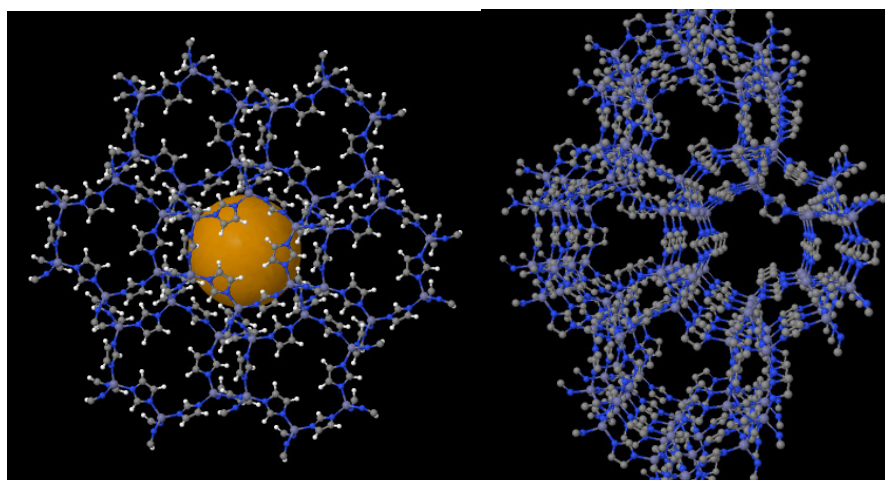
**Supporting Information Available:** XRD evolution with SOP cycles, SEM, ATR-FTIR, and wetting angle of ZIF-8 films.

#### 1. XRD evolution of films as the number of SOP cycles increases

In order to illustrate the evolution expected for X-ray diffraction patterns of ZIF-8 films deposited with increasing number of single-one-pot cycles (SOP), figure S1 is presented. It can be observed a comparison diffractograms obtained after 1x, 5x, 10x and 20x SOP performed using an APTES (primary amine) functionalized ITO coated glass, together with calculated diffractogram using known crystal structure and powder sample collected from supernatant present after every SOP cycle. Note that only after 10x SOP ZIF-8 expected peaks are fairly visible. Figure S2 display two views of ZIF-8 structure.



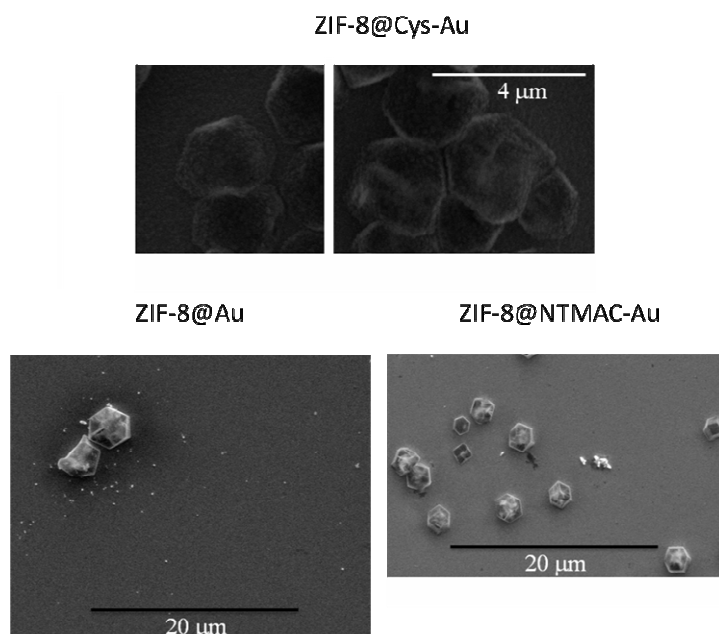
**Figure S1.** XRD corresponding to increasing number of SOP cycles, bulk ZIF-8 material, and calculated using known crystal structure.



**Figure S2.** Two views of ZIF-8 bulk material. Left image shows inner pore volume and right image channel lateral view.

## 2. SEM images for the different primers used on Au substrates

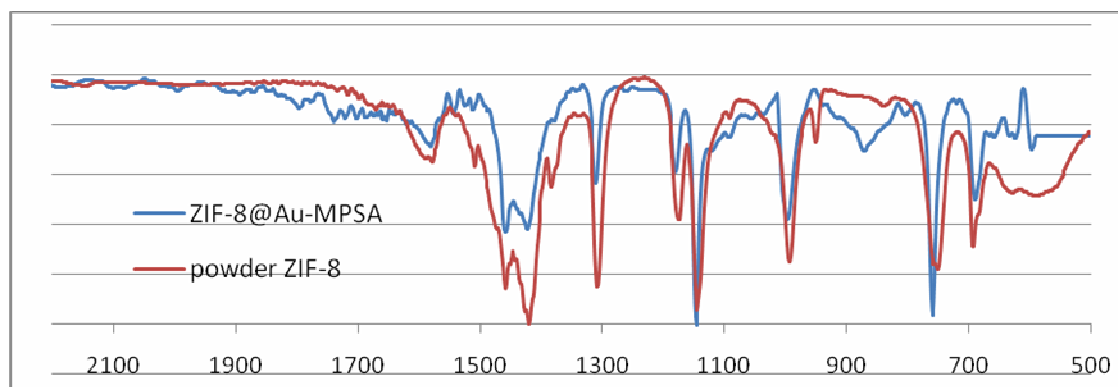
Figure S3 shows SEM images demonstrating the similarities of non-percolated PMAT and bare Au substrates, versus MPSA and Cysteamine modified percolated substrates as measured in CV experiments.



**Figure S3.** Additional SEM images showing similarities founded for MPSA/Cys modified substrates, and NTMAC/bare Au substrates.

### 3. Comparison of ATR-FTIR spectra taken from films vs. powder bulk samples

Figure S4 shows ATR-FTIR spectra taken using powder sample and films deposited over MPSA modified Au substrates.



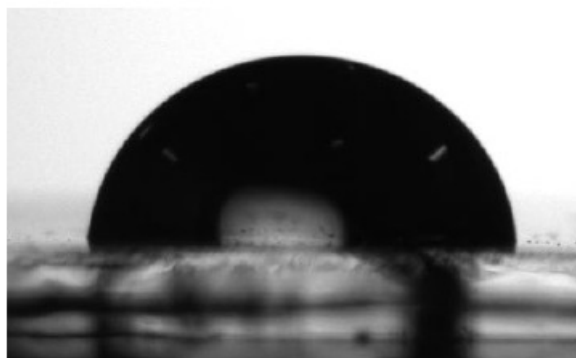
**Figure S4.** Comparison of ATR-FTIR spectra taken for powder ZIF-8 sample collected from supernatant of SOP and ZIF-8@Au-MPSA.

Figure S4 shows ATR-FTIR spectra taken from ZIF-8 powder sample and ZIF-8 films deposited on MPSA modified Au substrates. The perfect overlap between the spectra shows that both are related to the same chemical species and the absorption bands are in excellent agreement with that previously reported in literature for ZIF-8<sup>1-4</sup>. In particular, the band at 1590 cm<sup>-1</sup> is attributed to the C=N stretching, while those bands at 1460, 1430 and 1390 cm<sup>-1</sup> frequencies are attributed to the entire ring stretching. Bands at 1190, 1150, 1000 cm<sup>-1</sup> are associated to the in-plane bending of the ring, while bands at 1310 and 950 cm<sup>-1</sup> and those below 800 cm<sup>-1</sup> are associated to out-of-plane bending of the imidazole ring in ZIF-8.

### 4. Wetting angle of ZIF-8 films

Figure S5 shows wetting angle of films constructed using 5x SOP cycles over Au-functionalized substrates.

$85,5^\circ \pm 2$



**Figure S5.** Wetting angle measured for ZIF-8 films after 5x SOP cycles over Au functionalized substrates.

## 5. N<sub>2</sub> adsorption isotherms for bulk ZIF-8 material

Figure S6 shows Nitrogen adsorption isotherm for bulk powder material collected from supernatant present after every SOP cycle.

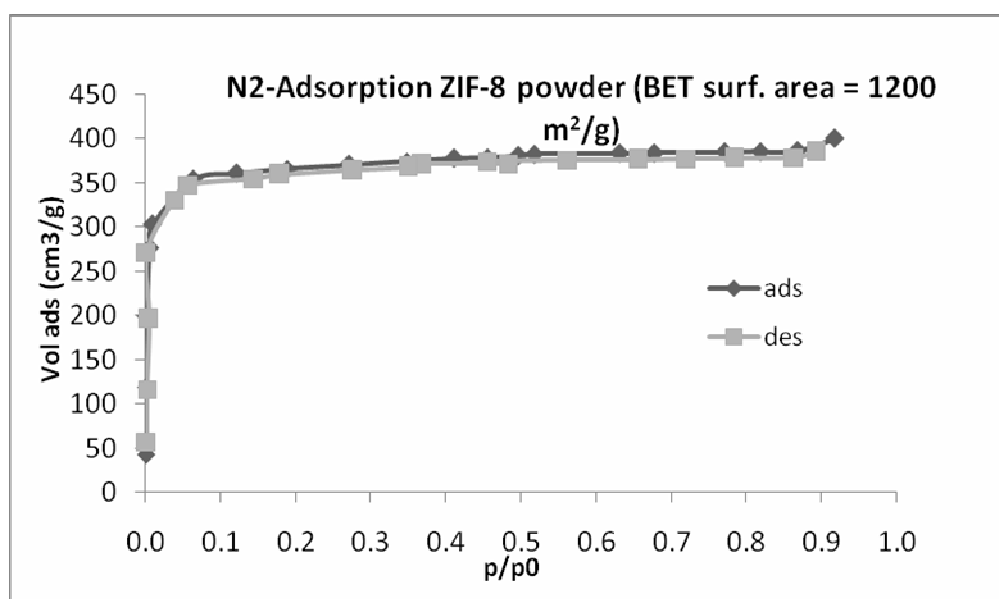


**Figure S6.** Nitrogen adsorption-desorption isotherm for ZIF-8 powder material collected from supernatant after SOP synthesis cycles.

## References

- [1] K. S. Park, Z. Ni, A. P. Côté, J. Y. Choi, R. Huang, F. J. Uribe-Romo, H. K. Chae, M. O'Keeffe, and O. M. Yaghi, *PNAS*, 2006, **103**, 10186–10191.
- [2] J. Yao, R. Chen, K. Wang, H. Wang, *Microporous and Mesoporous Materials*, 2013, **165**, 200–204.

[3] G. Lu and J. T. Hupp, *J. Am. Chem. Soc.*, 2010, **132**, 7832–7833.

[4] E. L. Bustamante, J. L. Fernández, J. M. Zamaro, *Journal of Colloid and Interface Science*, 2014, **424**, 37–43.